Prediction of interfacial behaviour of single flax fibre bonded to various matrices by simulation of microdroplet test

Shaima Bellil, Delphin Pantaloni, Darshil U Shah, Antoine Le Duigou, Christophe Baley, Johnny Beaugrand, Alain Bourmaud, Sofiane Guessasma

Composites Part C: Open Access 11 (2023) 100351

Contents lists available at ScienceDirect

Composites Part C: Open Access

journal homepage: www.sciencedirect.com/journal/composites-part-c-open-access

Prediction of interfacial behaviour of single flax fibre bonded to various matrices by simulation of microdroplet test

Shaima Bellil [a], Delphin Pantaloni [b], Darshil U. Shah [c], Antoine Le Duigou [b], Christophe Baley [b], Johnny Beaugrand [a], Alain Bourmaud [b], Sofiane Guessasma [a,*]

[a] UR1268 BIA, INRAE Nantes, BP 71627 Cedex 03, 44316 Nantes, France
[b] Universite Bretagne Sud, IRDL UMR CNRS 6027, IRDL, 56100 Lorient, France
[c] Centre for Natural Material Innovation, Department of Architecture, University of Cambridge, Cambridge, UK

ARTICLE INFO

Keywords:
Finite element method
Microdroplet test
Polymer
Flax fibre
Interfacial behaviour
Debonding

ABSTRACT

The microdroplet test is commonly used to determine the apparent interfacial shear strength (IFSS) of fibre-reinforced microcomposites. A deeper analysis of the test outcome can provide meaningful information about the fibre/matrix interface behaviour if a predictive approach is adopted. In this study, this predictive approach was used to investigate the quality of interface for polymer drops bonded single flax fibre at the microscale. Microdroplets of five thermoplastics matrices were prepared with single flax fibres. Microbond test was performed to assess the force–displacement curves of the studied composite systems. In addition, a finite element (FE) modelling methodology was adopted to quantify the interfacial role by proposing an interfacial constitutive law including the debonding stage. The numerical sensitivity results reveal the leading role of the interfacial stiffness as well as the fibre–matrix separation displacement in triggering the debonding behaviour. In addition, the numerical responses show strong matching with experimental trends using the proposed interfacial model for a wide variety of fibre/matrix interactions. The identification of the mechanical behaviour of the considered composite system shows that the best performing system is flax fibre/PLA, allowing a maximum fibre–matrix separation of 156 μm and an interfacial stiffness of 47 GPa/mm. The worst performing system is flax fibre/PP, which has a limited fibre–matrix separation of 55 μm. This study concludes that the proposed numerical model is able to capture the interfacial shear behaviour of polymeric drops bonded to a single flax fibre, which allows its extension at the mesoscale for a given arrangement of flax fibres in the bio-based composites.

1. Introduction

The growing interest in plant-fibre reinforced composites is pushing users to integrate them into an increasingly wide range of polymer matrices. This interest is motivated by the environmental issues caused by the use of synthetic materials such as glass fibres and difficulty to handle conventional composite end-of-life [1]. These developments are driven by the availability of new processes capable of manufacturing environmentally friendly products from bio-based or compostable matrices [2]. The performance of these bio-based composites is influenced by the intrinsic properties, the morphology [3], the length [4], orientation [5], defects [6], and the individualization of the reinforcing fibres [7]. This performance is also guided by the interface bond strength between the fibre and the matrix, notably the physical interactions or chemical bridging [8], which is believed to have a major effect on the breaking modes of the composite materials [9]. In addition, residual and internal hygro-stresses generate compressive stresses at the interface and possibly increase friction [10].

Improving the performance of composites reinforced by plant fibres is a complex problem to consider. At the bundle scale, the middle lamella strength is the weakest link and bundle breakage does not refer much to the fibre/matrix interface bond. When extrusion, injection or moulding is used, the effectiveness of the treatment after bundle separation can be questioned [11]. At the scale of the individual fibre, if the delamination of cell wall appears, fibre sizing can be questioned [12]. Besides these considerations, there is still room for improvement, by applying, for instance, fibre sizing, which is still referred as one way of improvement of adhesion with thermoset matrices. This way is effective in increasing, for instance, the interfacial shear strength (IFSS) by about 80% when mineral-based natural materials such as basalt fibres were

* Corresponding author at: UR1268 BIA, INRAE Nantes, BP 71627 Cedex 03, 44316 Nantes, France.
E-mail address: sofiane.guessasma@inrae.fr (S. Guessasma).

https://doi.org/10.1016/j.jcomc.2023.100351

Available online 23 February 2023

surface enriched in oxygen thanks to a plasma treatment, reflecting a performant fibre/matrix interface for the composite [13], or even radiation [14]. IFSS measurement by pull-out test are reported for plant fibres, like henequen with silane coupling agent [15] or for studying the retting bioprocess, mimicked by enzymatic treatment on hemp fibres [16]. The use of pull-out test is difficult at these dimensions because of the issues to set up a straight fibre embedded in the polymeric matrix. Based on previous investigations, the microbond pull-out test has proven to be more dependant of stress distributions along fibres due to geometry influence [9]. This is precisely one of the motivations behind conducting this work. In addition, the microbond test is perfectly adapted to the characterisation of the fibre-matrix interface for lengthy fibres such as glass, carbon, flax or hemp, as it allows the interfacial behaviour of the fibre to be obtained without the parasitic effects linked to slippage between fibres within a bundle. However, due to the geometry of this test and the need for a sufficient length, it is not suitable for most short fibres such as jute, sisal or palm fibres. In the case of hygroscopic fibres such as flax, the interfacial bond strength of natural fibre-polymer composites is sensitive to the hygroscopic behaviour especially under extreme water vapour environment [10], far from the usual 50% RH in testing setups. For instance, IFSS is reduced beyond 75%RH and improved below this limit. Others parameters like the fibre orientation efficiency factor, the fibre length efficiency factor or the critical fibre length are also reported to accurately simulate the stress-strain curves of fibre-based composites [17].

In order to characterise the performance of this interface, attempts have been made to compare the fitness of measurement methods [18] but there are currently no standardized methods to assess the interface quality in natural fibre reinforced composites [11] even if various approaches have been developed and are currently used in the academic and industrial communities. Macroscopic tests are possible at the composite scale (transverse tension on unidirectional composites or shear tests at $+/-45°$) [19,20] but microscopic tests such as the debonding of polymer microdroplets on an elementary fibre have shown their interest [21]. Indeed, these microscopic tests can be considered as simple configurations for the interface behaviour characterization. However, a full exploitation of these debonding tests requires a prior knowledge of the physical mechanisms and assumptions involved to explain the observed mechanical behaviour. This is particularly the case when the microdroplets break during the test or when flexible matrices, such as bio-based polymers, are used. For this case scenario, assumptions are usually made about the strength of the drop and its possible deformation during the test.

A former experimental study by the research group has shown various apparent shear strengths exhibited by polymer drops bonded to flax fibre measured by microdroplet testing [22]. In the present work, we determine the interfacial behaviour of various thermoplastics drops bonded to single flax fibres through the simulation of the microdroplet test using finite element method. This method has been considered to study the interfacial behaviour in varieties of materials such as carbon, glass as well as natural materials [23–26]. Flax fibres are combined with a selection of thermoplastic polymers matrices with contrasting mechanical properties and behaviour. The first part of this study is dedicated to the interpretation of the experimental microdroplet test. The second part deals with the implementation of a numerical approach that proposes a new interpretation of the relationship between the reaction force and the fibre displacement based on an interfacial constitutive law. A 2D finite element model was implemented for this purpose on the basis of experimental analysis where the fibre–matrix interface is considered as a zero-thickness elastic layer. The identification of interfacial and geometrical parameters and the interpretations of experimental/numerical load-displacement curves are discussed in light of the numerical results.

2. Materials and methods

2.1. Materials

Elementary flax fibres were extracted manually from the Flaxtape® unidirectional preform provided by Ecotechnilin company (Yvetot, Seine-Maritime, France); the reinforcement preform is made of a mix or several batches of textile flax fibres, cultivated and dew-retted in Normandy (France), between March and August 2019 (Fig. 1a-b). Single fibres were manually extracted and bonded to cardboard supports. Five polymers were used as a matrix for the debonding test: poly-(lactid) (PLA), poly-(hydroxyalkanoate) (PHA), poly-(butylene-succinate) (PBS), poly-(propylene) (PP) and maleic anhydride grafted poly-(propylene) (MAPP) + poly-(propylene) (PP). The selection of the biopolymeric matrices was guided by the differences in the mechanical properties (Table 1), where PP and MAPP are used as references.

2.2. Microbond sample manufacturing

Microbond sample manufacturing and debonding characterization were performed following a protocol adapted for thermoplastic and thermoset polymers in [27] and [28], respectively. The micro-droplet sample preparation consists of fixing manually a polymer wire, obtained by melting and rapidly stretching polymer films, to an elementary flax fibre by making a double knot around the fibre (Fig. 1c). Finally, the system was put in an oven for 8 min at 200 °C to melt the polymer double knot and transform the fibre/matrix into a microdroplet as illustrated in Fig. 1d. The symmetry of the microdroplet is checked and then the dimensions were carefully measured using an optical microscope (Olympus). The geometrical characteristics of each system (length and diameter of droplet and fibre diameter) were calculated by averaging several measurements. The droplet aspect ratio was then obtained by dividing the droplet average length by the radius. Fig. 2 depicts typical microdroplet configurations according to the five composite systems. Table 2 shows the averages and standard deviation values of geometrical features measured for each considered composite system. In addition to these features, parameters of the interfacial debonding law are provided. These are such the interfacial stiffness ($K0z$), the debonding propagation rate (az), the maximum fibre–matrix separation displacement (δ_d), and the non-linearity factor (f). The definition of these parameters and their implementation is given in the modelling section.

2.3. Mechanical testing

The microbond test of the flax fibre embedded in polymeric matrices is performed according to the method described in [22]. The elementary fibre/micro-droplet system was placed in a tensile machine equipped with a 2 N load cell. The fibre is placed between two razor blades with the droplet just below them (Fig. 3). The fibre is pulled at a displacement rate of 0.1 mm/min, starting with the blades locking the droplet, and continuing until debonding occurs. The droplets that were heterogeneous, asymmetrical, too small or too large compared to the average of the droplets produced were discarded from testing in order to eliminate most of the effects induced by differences in drop geometry. Load–displacement curves were obtained for all studied composites. For each polymer, at least 20 samples were tested to calculate the mean interfacial shear strength (IFSS). IFSS is commonly obtained using Eq. (1), where F is the debonding force, L_d the length of the droplet and D_f the diameter of the fibre [2,22]. The apparent shear stress is obtained by considering the constant shear stress along the embedded zone according to the Kelly-Tyson's hypothesis [29]

$$IFSS\ (\mathrm{MPa}) = F(\mathrm{N}) \big/ \pi \times L_d(\mathrm{mm}) \times D_f(\mathrm{mm}) \quad (1)$$

where F is the debonding force, L_d is the length of the microdroplet and

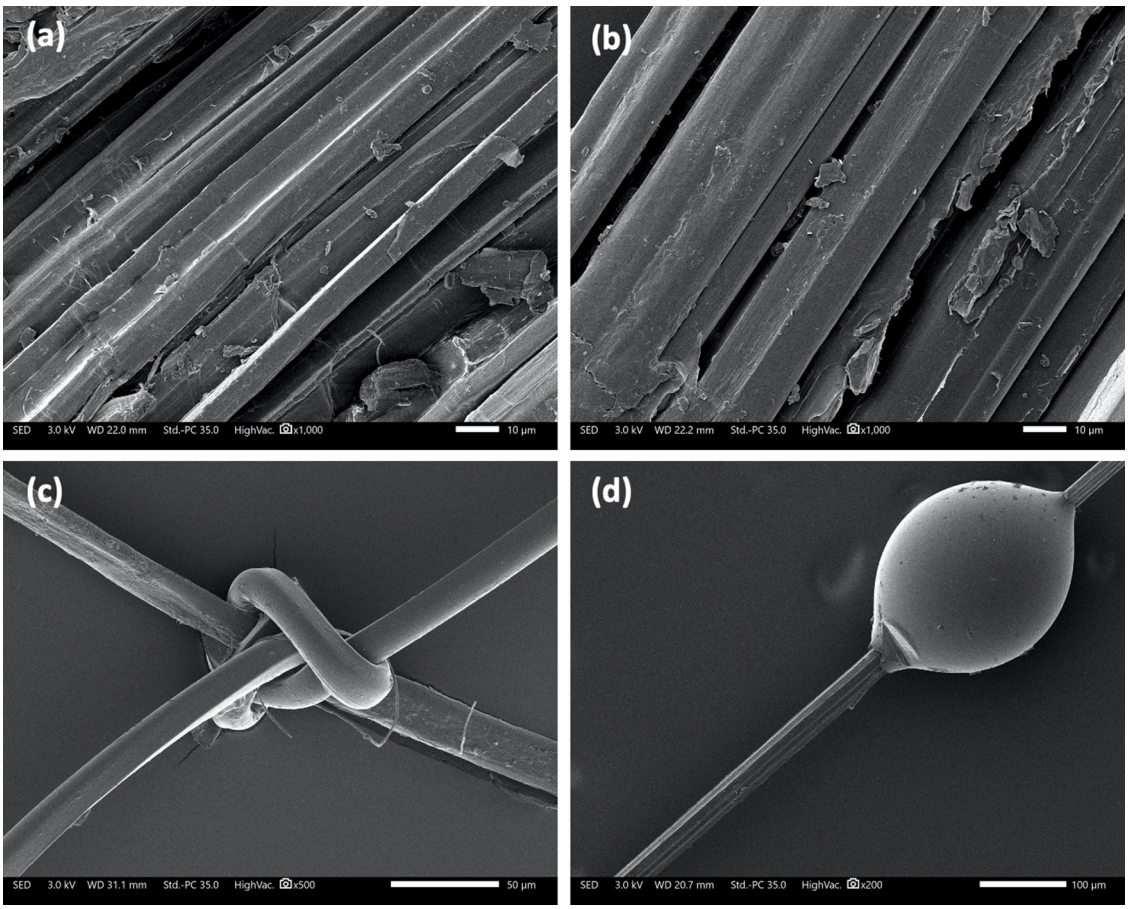

Fig. 1. (a, b) Morphology of flax fibres, (c) example of a double knot of PLA around a single flax fibre and (d) a microdroplet of PLA on a flax fibre.

Table 1
Polymeric matrix and flax fibre mechanical properties [21].

Property*	Flax fibre	PLA	PHA	PBS	MAPP	PP
ρ (g/cm^3)	1.45–1.50	1.24	1.25	1.26	0.934	0.855
E (GPa)	52.5 ± 8.60	3.8 ± 0.1	4.4 ± 0.3	0.75 ± 0.10	1.58 ± 0.05	1.4 ± 0.20
σ_r(MPa)	945 ± 200	61.4 ± 0.8	38.6 ± 1.4	39.1 ± 0.5	25.1 ± 0.1	24.4 ± 0.8
ν (-)	0.48	0.4 ± 0.02	0.40	0.47	0.4	0.4
ε_r(%)	2.07±0.45	2.0 ± 0.10	1.3 ± 0.10	14.7 ± 5.40	5.3 ± 0.20	4.3 ± 0.70
IFSS (MPa)	-	15.6 ± 2.7	8.3 ± 1.1	8.5 ± 1.5	9.8 ± 1.8	4.6 ± 0.6

σ_r : density, E : Young's modulus, σ_r : Rupture stress or ultimate stress, ν : Poisson's coefficient, ε_r: elongation at break

D_f is the diameter of the fibre.

In our case, the IFSS is determined graphically from the slope of the shear force-bonded surface according to the approach proposed by Miller [21,22].

2.4. Finite element computation

The finite element modelling is adopted to derive the constitutive law of interfacial debonding that quantifies the observed composite behaviour. The modelling is considered using the mechanical module from the Comsol Multiphysics (version 5.6), which reproduces the testing conditions of a typical microdroplet test. COMSOL Multiphysics is a numerical simulation software based on the finite element method. This software allows solving numerically the partial differential equations of the considered structural problem and finding the stress and strain distribution thanks to a discretization of the computation domain. The structural mechanics module of the Comsol Multiphysics software has been successfully used to solve the pull-out problem for metallic fibres embedded in polymeric matrices to predict the polymer–metal interfacial behaviour [30]. Parameters are set according to five steps: geometry and meshing, constitutive laws of the phases in the composite including the interface parameters, the boundary conditions corresponding to the considered mechanical test, the type of analysis and post-treatment of the results. These are further detailed in this section.

All geometric parameters are adjusted according to the microdroplet experiments (Fig. 4a). It has to be mentioned that the interface properties can be introduced through either a thick layer called interphase [31] or by considering a zero-thickness interface layer [32]. This last approach is considered to achieve a more precise stress distribution across the interface. This is due to the fact that interphase response corresponds to an average of phase and interface responses across the interphase thickness. The mechanical behaviour of plant fibres is known to vary depending on several factors such as the fibre diameter and the density of the defects [3]. Using one average experimental curve as a basis for comparison with the numerical results would be limited to achieve a robust predictive analysis of the interfacial behaviour. In order to be consistent with geometry variability, especially the polymeric droplet size and the flax fibre diameter, simulations were run based on five replicates per each flax fibre/polymer system instead of using average values.

The droplet shape is assumed to be ellipsoid with a diameter and length adjusted according to Fig. 3. The approximation accounts for the junction between the fibre and the droplet where the geometry

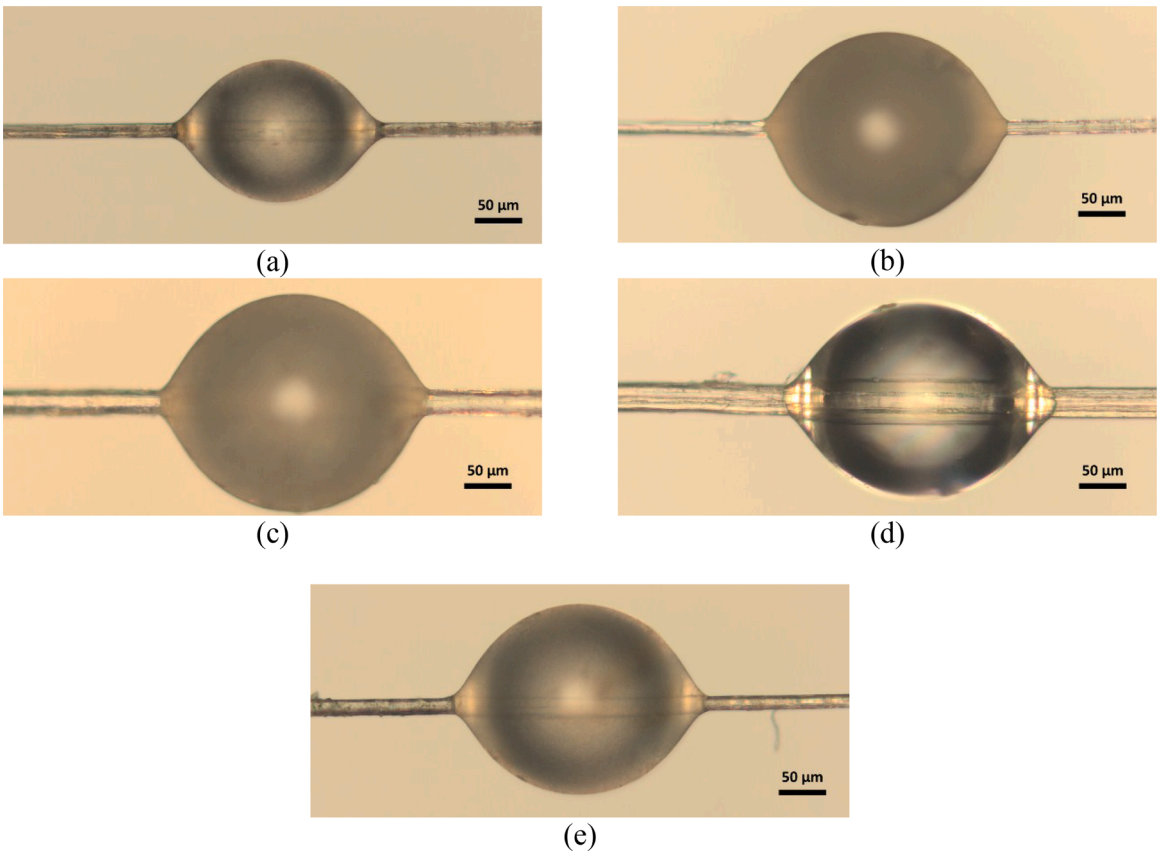

Fig. 2. Flax/ polymer microdroplet systems for the microdroplet test: (a) flax fibre/MAPP. (b) flax fibre /PBS, (c) flax fibre /PHA, (d) flax fibre/PLA, (e) flax fibre/PP.

Table 2
Predicted parameters of the interfacial debonding law for single flax fibres bonded to five polymeric drops.

Parameter	PLA	PHA	PBS	MAPP	PP
D_d (µm)	155 ± 32	151 ± 53	191 ± 42	162 ± 15	159 ± 23
L/D_d (-)	1.29 ± 0.04	1.32 ± 0.16	1.26 ± 0.05	1.36 ± 0.05	1.39 ± 0.8
D_f (µm)	23 ± 7	22 ± 9	17 ± 3	21 ± 6	18 ± 2
Δ_{IFSS} (%)	2.39 ± 1.96	1.67 ± 1.24	1.19 ± 0.58	0.41 ± 0.27	1.88 ± 1.09
$k0z \times 10^9$ (N/mm^3)	47 ± 12	57 ± 17	59 ± 13	53 ± 14	55 ± 8
δ_d (µm)	156 ± 61	78 ± 23	82 ± 15	107 ± 23	57 ± 7
$a_Z \times 10^6$ (mm^{-1})	2.0 ± 0.00	0.65 ± 0.35	2.0 ± 0.00	0.95 ± 0.41	1.00 ± 0.09
f (-)	0.49 ± 0.14	0.49 ± 0.08	0.46 ± 0.08	0.19 ± 0.06	0.41 ± 0.03

K0z : Interfacial stiffness, *az*: debonding propagation rate; δ_d : maximum fibre–matrix separation displacement; *f*: non-linearity factor.

quantifiers of the droplet are measured after the solidification completion. The slight differences between the real and simulated geometries can induce relatively small changes in the contact area between the blades and the droplet and thus the exerted force on the droplet may slightly vary. The elliptical shape approximation still holds as the induced change in the contact area is nearly the same for all the polymeric systems.

The flax fibre is, however, approximated as a cylindrical feature (Fig. 4a). Thus, according to these geometrical considerations, the symmetry of the problem allows using a 2D axisymmetric model to reduce the computational duration. The diameter of the fibre was found to vary between 11 µm and 28 µm with a typical length of 500 µm. In addition, the length of the microdroplet varied between 131 µm and 288 µm and its diameter varied between 84 µm and 238 µm. The variability in microdroplet size is difficult to control experimentally. However, the model is able to handle such variability through the ellipsoid geometry.

An isotropic elastic model is considered for both materials, where elastic modulus, E and Poisson's ratio, *ν*, are implemented for the flax fibre and the polymeric matrix according to experimental data summarized in Tables 1 and 2, which are also reported in [2].

A mesh convergence study was undertaken to determine the optimised mesh that capture rapid changes in stress and strain distributions while keeping the computation time reasonable. The convergence for all tried meshes is ensured even at the point where the flax fibre is extracted from the polymeric matrix. The meshing was varied from coarse to extremely fine allowing a total number of elements between 128 up to 2958 elements, and an average element size between 1 µm and 15 µm (Fig. 4b). Preliminary analysis of the strain distributions such as the shear strain component e_{xz} shows that meshes above coarse level are sufficient to capture strain and stress gradient within the system. In addition, negligible variation in the overall force–displacement response is observed for all meshes. Thus, an extremely fine mesh is considered for all computations. This mesh consisted of 2958 triangular quadratic elements is adopted as shown in Fig. 4. Triangular meshes are used because of the higher symmetry compared to quad meshing allowing to tesselate more efficiently the 2D domain. In addition, quadratic elements are used over linear ones to achieve more accurate results because of the use of non-linear shape functions where displacements between the nodes are interpolated using a higher order polynomial function. According to this scheme, each element is described by three nodes and each node has 2 degrees of freedom (dof) corresponding to structural displacements in the radial (R) and axial (Z) directions (UR, UZ).

The boundary conditions consist of a top end of the fibre subjected to an imposed displacement with a constant rate in the loading direction, while the top of the droplet is constrained against displacement to

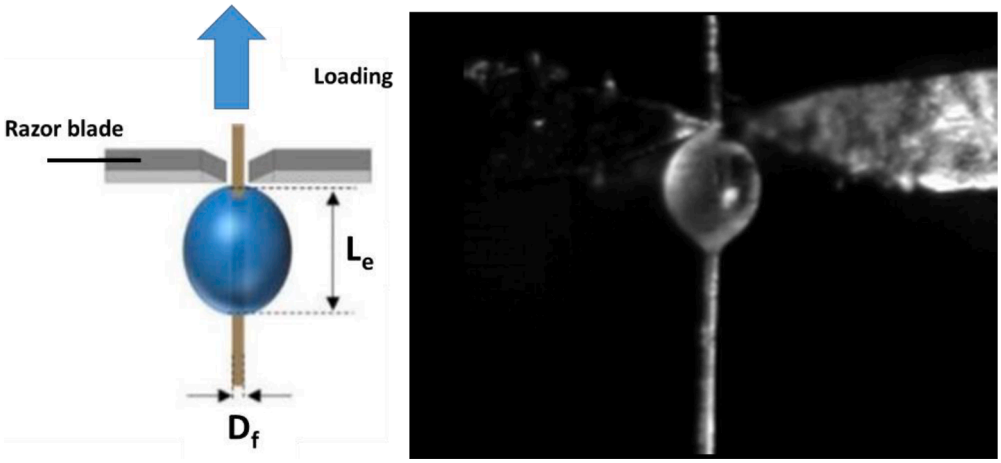

Fig. 3. Microdroplet test illustrations showing the fixture and geometrical parameters.

simulate the blocking effect of the blades. The fibre–matrix interaction is represented as an interface with a stiffness value of $K0z$. This parameter is identified from the comparison between the experimental and numerical responses.

The interfacial behaviour is modelled using Eqs. (2) and (3). When the interfacial displacement jump does not exceed the maximum separation δ_d value, the interfacial behaviour is linear and corresponds to a spring-like response with the interfacial stiffness $k0z$.

$$F(N) = k0z \times x;\ 0 \le x \le \delta_d \tag{2}$$

The debonding at the fibre–matrix occurs when the load reaches a critical value [30], and corresponds to a descending trend in the force–displacement response. In this study, an exponential function was used to capture the interfacial debonding:

$$F(N) = (k0z * (1-f) \times \exp(-az \times (x-\delta_d)) + f \times k0z\ ) * \delta_d;\ \delta_d \le x \le \delta_s \tag{3}$$

where $k0z$ is the interfacial stiffness of the interface per unit length, a_z is a parameter that represents the debonding propagation rate of the fibre-matrix interface. x is the separation displacement or displacement jump across the interface, δ_d represents the critical separation displacement, δ_s is the maximum separation displacement and f is a factor that provides the balance between an exponential-like and linear-like force decreasing trend. Both $k0z$ and δ_d are physical parameters whereas the rest of the parameters (a_z, f) can be considered as fitting parameters.

The quasi-static problem with displacement increments was solved using a direct solver. More than 60 runs were needed to conduct parameter sensitivity analysis and identification based on the matching between numerical and experimental force - displacement curves.

3. Results and discussion

3.1. Experimental results of microdroplet test

The five composites systems are tested under the same conditions (i.e., similar setup and comparable droplet configurations) to be able to draw meaningful conclusions about the interface contribution in each case on the overall mechanical response. Although, microdroplet test is not comparable to a pure shear test, the overall shear behaviour can still be captured. For all considered systems, the damage mechanism explaining the failure is the interfacial shear failure for all polymers. Fig. 5a illustrates the force–displacement curve of a typical microbond test of a flax fibre based composite material. The interface behaviour representing the fibre/matrix shear interaction affects the overall mechanical response according to a four-stage process. The first stage corresponds to a linear increase of the force and involves the elastic response of the interface. The slope of the linear part depends mainly on the phase properties and the interfacial stiffness. However, the quasi-elastic behaviour of the flax fibre/polymetric matrix composite indicates that there is no progressive damage growth that can be expected as a deviation from the linear increase especially close to the peak force. This distinctive feature of the studied composites narrows the damage initiation to the location at the peak force, which can be referred to as a second stage. This stage marks the crack initiation from the top position where stress concentration develops and triggers interfacial crack departure. The next stage corresponds to the development of damage by instable crack propagation, which is responsible for the drastic decay of the force as shown in Fig. 5a. This third stage of the pull-out process is followed by a frictional sliding due to fibre roughness and residual stresses. This stage occurs along the loading direction where residual force partially resists the flax fibre pull-out. The extend of the pull-out stages is material dependent and allows different ranking of the interfacial properties. Indeed, the experimental results of IFSS shown in Table 1 suggest that flax fibre / PLA composite has the best interfacial properties. Both PHA and PBS results in a similar ranking while PP corresponds to the worst system to blend a flax fibre with. This means that all systems based on biopolymer matrices have better compatibility with flax fibre compared to MAPP and PP. A former study by the research group attributes this ranking to the high surface tension observed for PLA/PHA/PBS [22]. In addition, bonding between flax fibre and the biopolymer systems is facilitated by the presence of ester groups where hydrogen bonds strongly improve the adhesion properties with most of the system except for PP. The observed ranking of the IFSS values has a direct consequence on the macroscopic transverse strength of the composites. As shown in a previous research work [22], Among the four flax-thermoplastic systems, flax fibre / PLA composite exhibits the highest transverse tensile properties compared to the other composites, in a similar way to what has been observed at the microdrop test scale. This correlation between interfacial properties obtained by micro drop test and macroscopic properties such as shear tests on bi-axial composites has also been demonstrated on bio-based epoxy resin systems [33].

3.2. Numerical results: sensitivity analysis

Fig. 5b shows the typical predicted von Mises stress counterplots as a function of an increasing load for the system flax fibre / PLA composite. This quantity is a good indicator about the stress concentration and it is used more to show the regions where the high stress levels are present rather than how the yielding occurs. A supplementary material is provided as an animated sequence showing both the predicted stress evolution and the corresponding real microdroplet test for the same

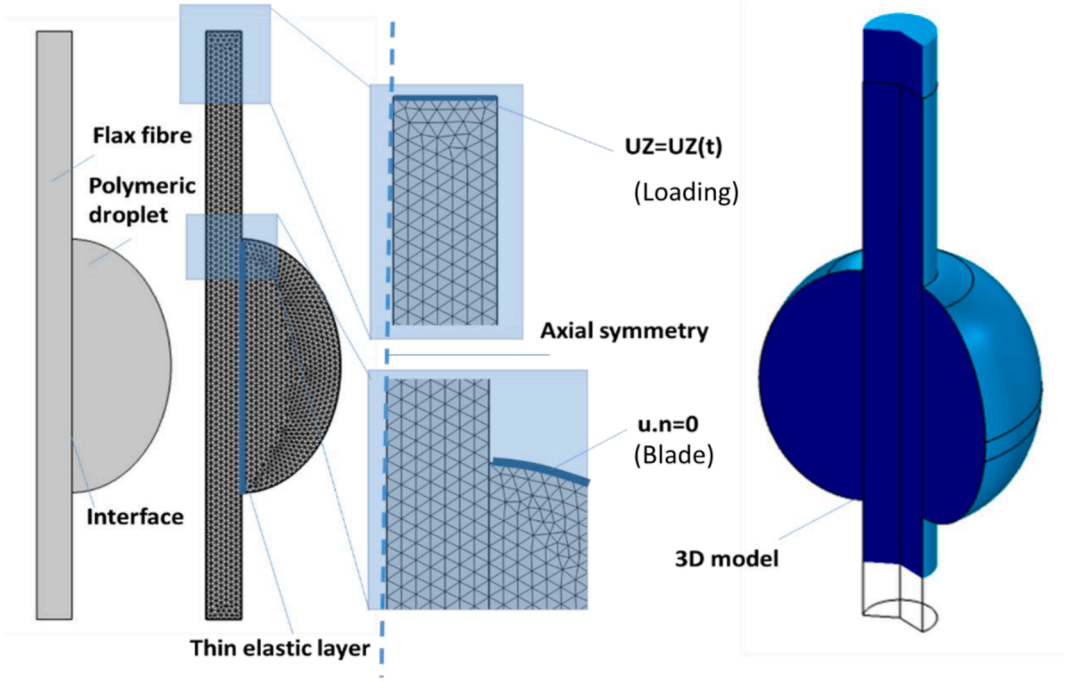

(a)

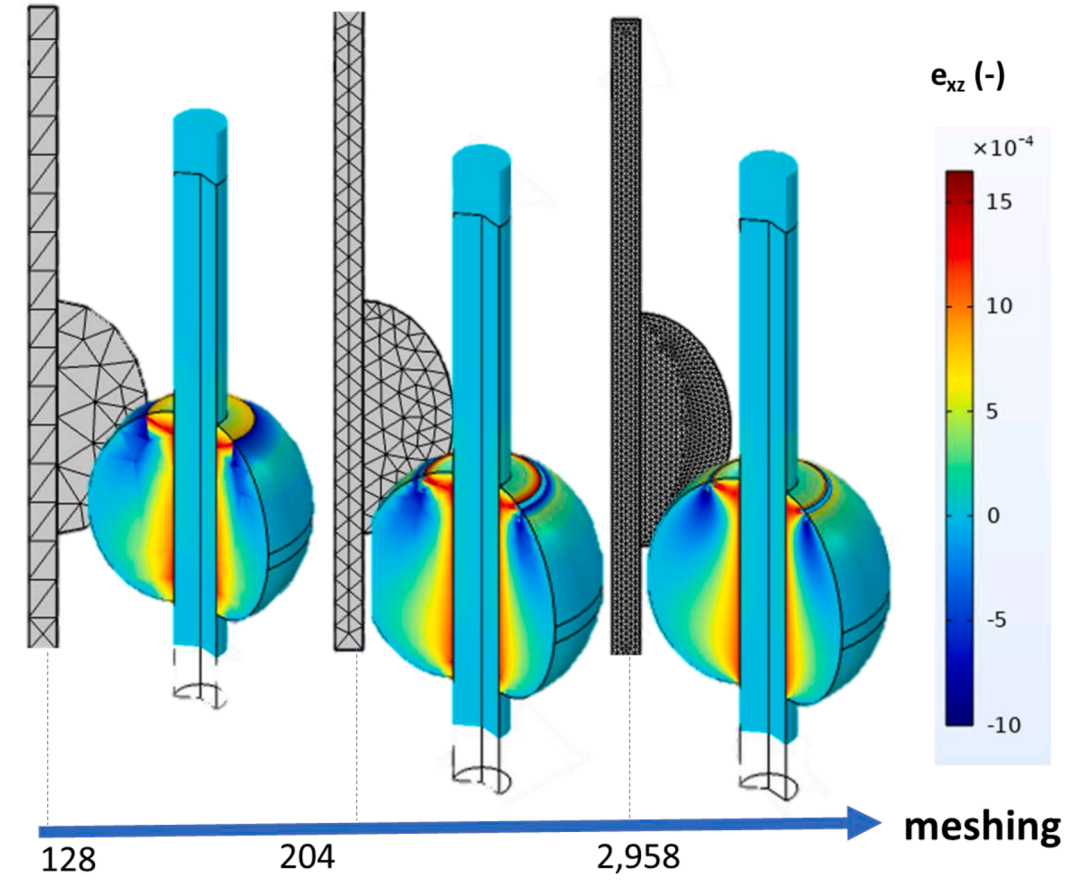

(b)

Fig. 4. (a) Illustration of the geometry and meshing used in the finite element computation, (b) mesh study showing the effect of the element size on the shear strain e_{xz}.

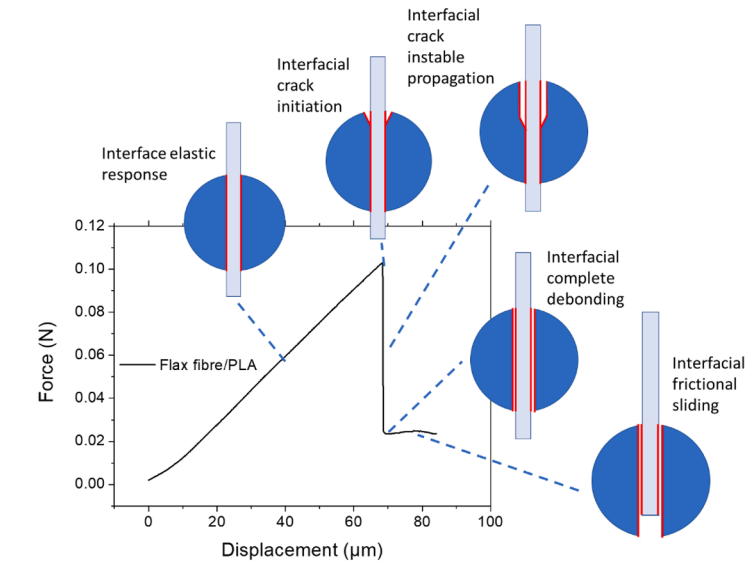

(a)

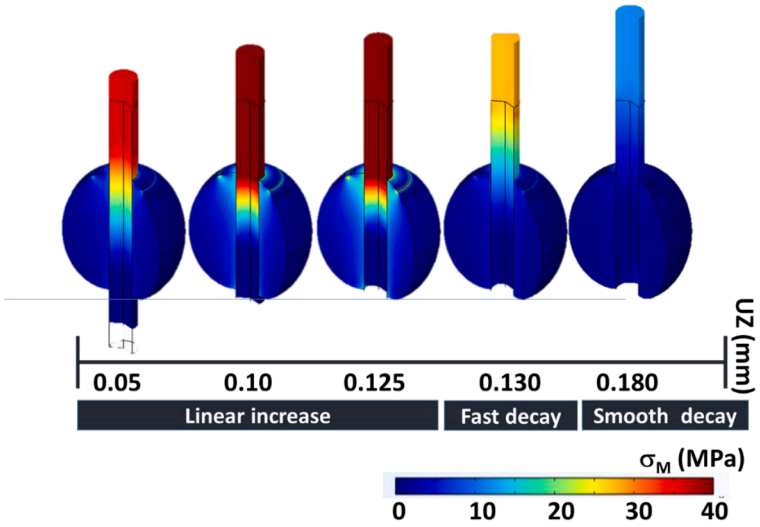

(b)

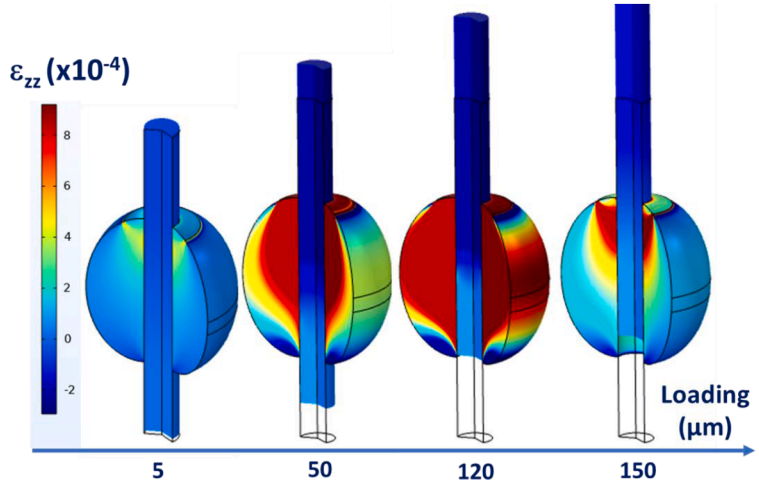

(c)

Fig. 5. (a) Schematic of the pull-out load–displacement curve with key stages describing the interface behaviour, Typical (b) von Mises stress (σ_M), and (c) normal (ε_{zz}) strain components showing the main deformation stages of microdroplet test for flax fibre / MAPP composite.

condition (flax fibre/PLA composite). Fig. 5b captures the stress state associated with the main stages described in the previous section. The linear increase of the force corresponds to regular increase of the stress levels in the microdroplet. However, this increase is not homogeneous in the droplet. Stress concentration occurs at the vicinity of the fibre / matrix interface and extends, with lower levels in the inner core of the microdroplet. This stress concentration occurs as a result of the displacement constraint applied by the blades, where part of the overall stress is transferred to the interface. This load transfer acts against the work of adhesion up to the limit described by the critical separation displacement δ_d. Fig. 5c illustrates the generated deformation in the loading direction by considering the counterplot of the normal strain component (ε_{zz}) in the z-direction. From the first load increment of 5 μm up to the loading value of 120 μm close to the peak force, the strain distribution continuous to increase within the core of the droplet. At the peak force, Fig. 5c demonstrates that the largest load transfer is reached because the entire interface is under large strain state. Debonding occurs according to the scheme described by Pisanova et al. [34], where the interface stiffness rapidly decreases. This can be read from the decrease of large strain levels within the polymeric droplet (Fig. 5c). The loss of interfacial stiffness results in the fast decay of the force, and marks the initiation and crack development along the flax fibre / polymeric matrix interface. Within these stages a sudden decrease of the stress levels down to 20 MPa is predicted for the case of MAPP (Fig. 5b). When the force reaches a steady value, a smooth decay trend corresponds to the decrease of the stress levels in the direction of loading as a result of the complete interface debonding. For loading values beyond 150 μm, the largest strain levels are restricted in the region close to the blades (Fig. 5c). This trend is mainly affected by the fibre length. In Fig. 5b, the fibre length is considered as finite, which results in a low contact area as the fibre passes through the microdroplet. In reality, the fibre length can be much larger causing the force to maintain its trend as long as the loading continue. In the present case, the fibre length can be as large as a four time the microdroplet size. The final stress state within the microdroplet reflects the minimum force value achieved after testing. This zone corresponds to the result of fibre–matrix friction, which occurs along the flax fibre length and affected by several factors such as the fibre roughness, the difference between Poisson's ratios of the matrix and the flax fibre [27].

In order to identify the role of the interfacial parameters considered in the debonding law (Eq. 2), namely the stiffness $K0z$, the debonding propagation rate az; the maximum fibre–matrix separation displacementδ_d, and the non-linearity factor f, a sensitivity analysis is conducted in the case of flax fibre / PLA composite.

In order to proceed with the sensitivity study, a reference condition is selected, which reflects typical experimental responses: k0z = 36, 3 GPa/m, $az = 2.10^6 mm^{-1}$, $\delta_d = 0.136$mm and $f = 0.69$. As for the geometry of the Flax fibre / PLA system, the fibre and microdroplet diameters are 28μm, and 158μm, respectively. The microdroplet length is adjusted to 216μm for which the aspect ratio $\frac{L_d}{D_d}$ is 1.364. It has to be mentioned that the ratio between the critical displacement δ_d and the microdroplet diameter D_d is high for this reference condition.

Fig. 6 illustrates the individual effect of the debonding law parameters based on four different levels of variation, taking as a case study the

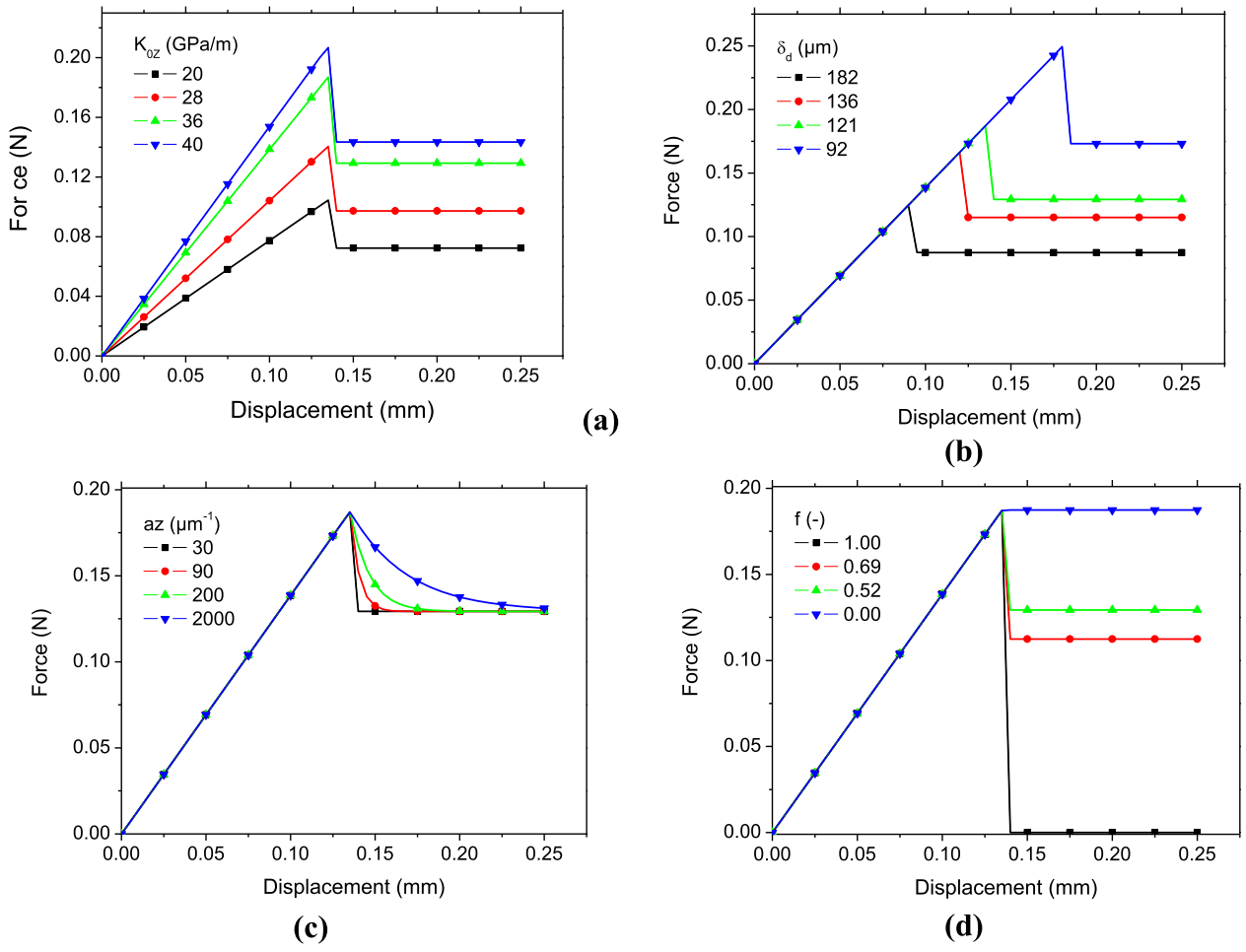

Fig. 6. Sensitivity analysis of the interfacial debonding law in PLA/flax system. Effect of (a) interfacial stiffness, (b) fibre–matrix complete separation displacement, (c) debonding propagation rate, (d) non-linearity factor.

flax fibre/PLA system. Fig. 6a shows that the interface stiffness linearly influences the overall slope of the load–displacement response as well as the peak force value. In fact, $k0z$ can be identified irrespective of the other parameters by matching the slope of the numerical curve to the experimental one. Here, the stiffness of the blade is not considered, which may interfere in the intensity of the load transfer. This alteration can be considered as negligible due to the large contrast between the composite stiffness and the blade properties.

Among the other significant parameters, δ_d has an interesting effect on the predicted force–displacement response. In fact, it does not affect the slope of the response but the peak force instead, without modifying the overall shape of the decreasing branch as illustrated in Fig. 6b. $\delta_d$helps mainly in finding numerically the debonding force. The larger δ_d is, the higher the force is required for initial debonding. In addition, the area under the curve represented by the interfacial force versus the displacement jump corresponds to the work of adhesion needed to trigger the debonding. When the maximum force is eventually reached, the debonding is completed and the frictional sliding stage takes place. The overall shape of the decreasing branch of the loading curve varies depending on the debonding propagation rate az as shown in Fig. 6c. This parameter modifies the profile from an exponential to a linear one.

Fig. 6d shows the remarkable effect of the non-linear factor f on the frictional sliding. This parameter varies in its entire range between 0 and 1. In fact, when the complete decohesion occurs, the force reaches a plateau value that f is able to capture. It has to be mentioned that at its maximum level, the observed behaviour depends on the other parameters of the debonding law. For instance, in Fig. 6d, the residual force matches the maximum one, which does not allow to observe the non-linear decay captured in Fig. 6c. When f is grounded, the linear decreasing trend takes place and again the profile of the curve depends on the levels of the remaining debonding parameters. The analysis of the deformation stages identified in Fig. 5b and the sensitivity analysis in Fig. 6 show that the interface stiffness influences the first stage, the critical separation displacement affects both the first and second stages, whereas the debonding propagation rate and the non-linearity factor influences the third stage.

In addition to the sensitivity of the microdroplet test to the interface debonding law, the geometry of the flax fibre / polymeric system is studied by varying the fibre and microdroplet dimensions (Fig. 7). It is found that the microdroplet aspect ratio, the fibre and microdroplet diameters show global effects on force–displacement response because the slope, maximum force and the decay trends are all affected. However, the magnitude of the effect and its rate depends on the selected window for the geometric parameters. In addition, the distance between the razor blades during debonding may affect the stress distribution. However, this effect is not considered in this study since the number of nodes constrained at the top of the droplet is kept constant.

For instance, when the flax fibre diameter is varied between 19 μm

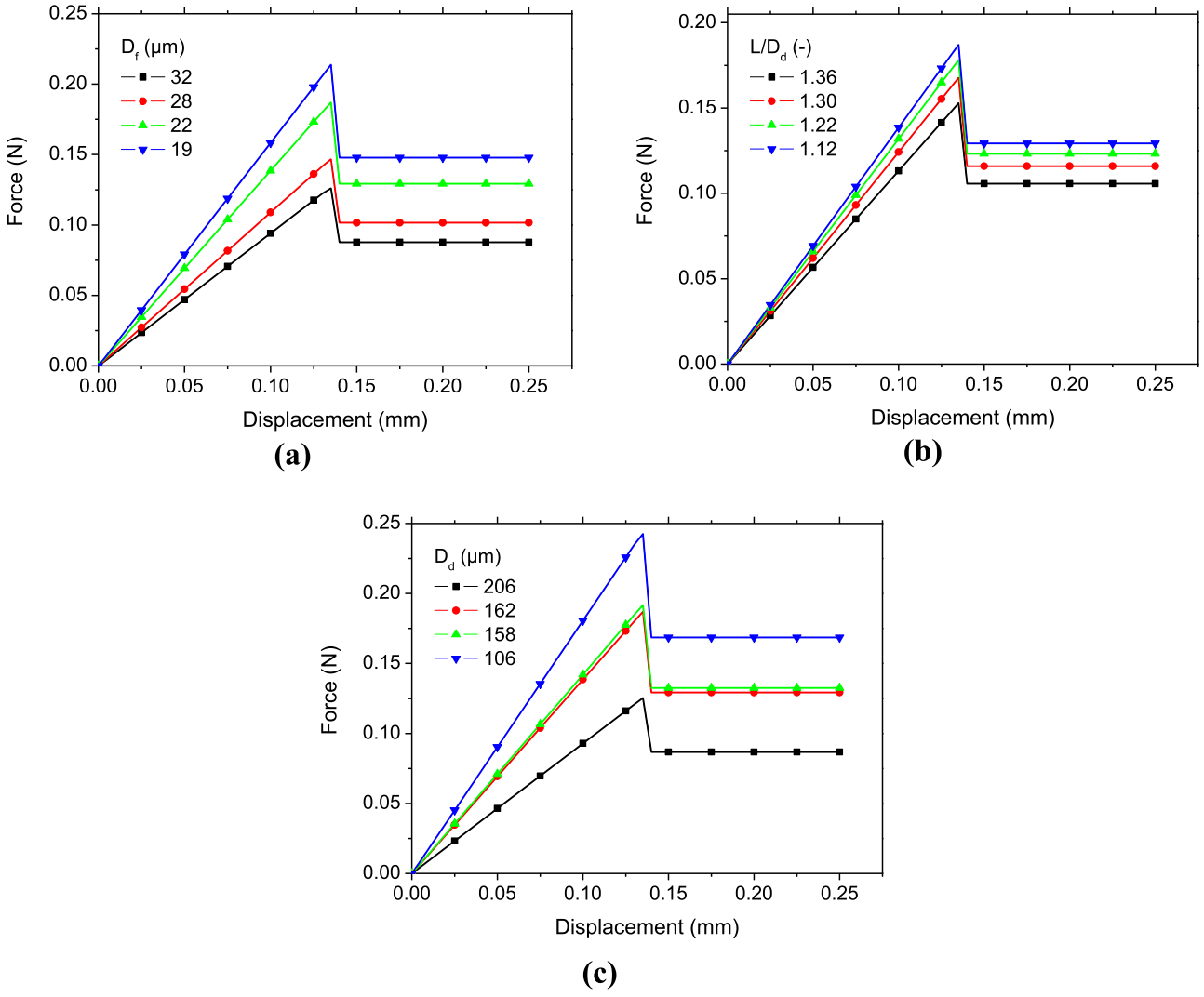

Fig. 7. Sensitivity analysis of the geometry consideration in PLA/flax system. Effect of (a) flax fibre diameter, (b) aspect ratio between the diameter and length of the microdroplet, (c) microdroplet diameter.

and 32 μm (Fig. 7a), the maximum force nearly doubles. This effect is associated to the increase of the surface area of the flax fibre that generates larger reaction forces for the same amount of loading. The same explanation still holds for the microdroplet diameter and aspect ratio as these parameters influence the contact surface between the blades and the microdroplet (Fig. 7b, 7c).

The results illustrated in Figs. 6 and 7 demonstrate the capability of the finite element model to capture different scenarios of damage initiation according to the interfacial debonding expression (3). In addition, all stages of the interfacial failure mechanisms are considered

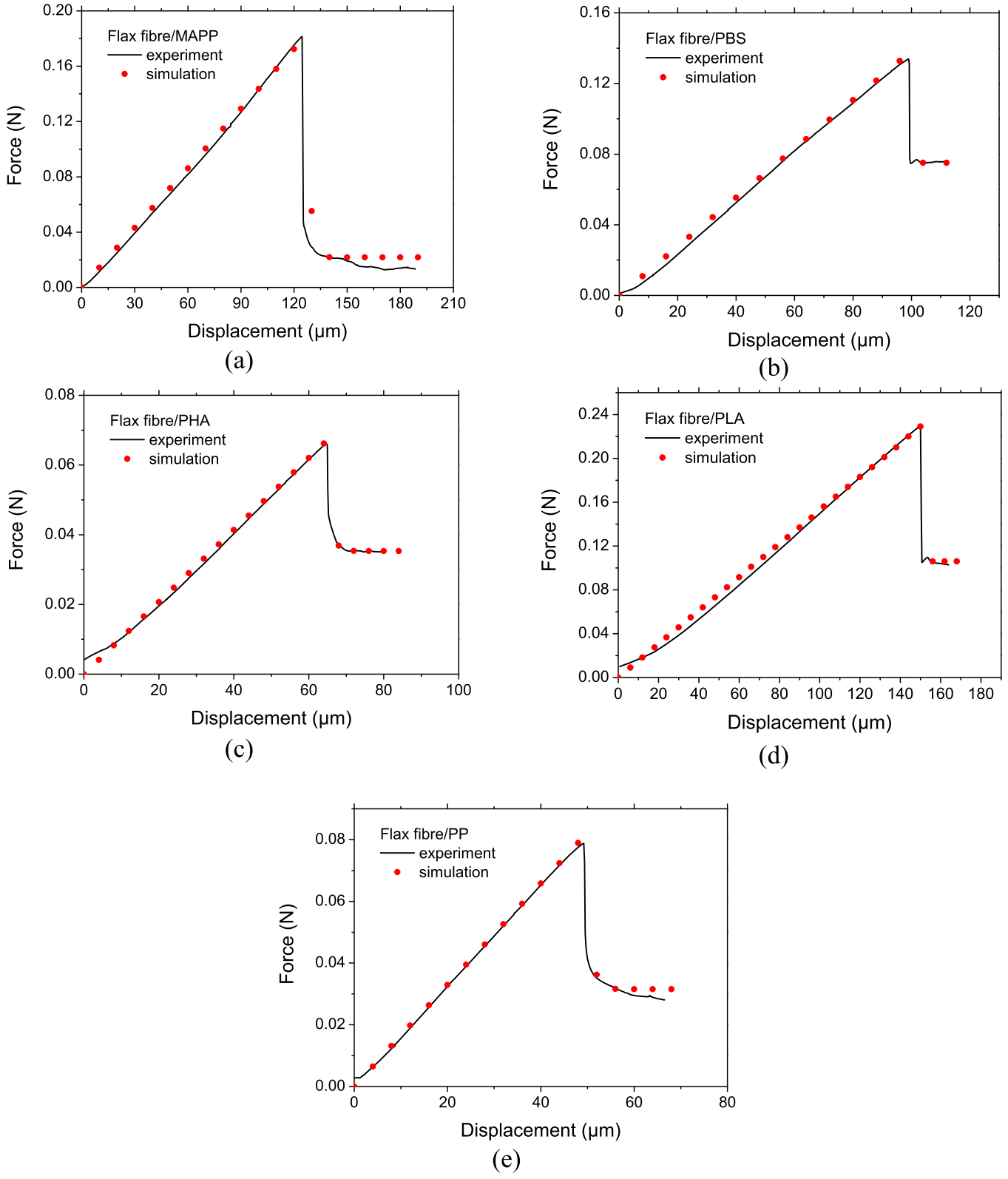

Fig. 8. Comparison between experimental and numerical responses of the studied composites based on identified set of parameters of the debonding law: (a) flax fibre/MAPP. (b) flax fibre /PBS, (c) flax fibre /PHA, (d) flax fibre/PLA, (e) flax fibre/PP.

including the elastic, cracking, debonding and sliding stages [35]. Bahl et al. [36] considered another alternative using a cohesive model to capture the properties of fibre–matrix interface in fibre reinforced metal matrix composite. Although, their model is able to capture interfacial damage initiation at different nominal stress values when the deformation is purely in the shear direction, the cohesive model does not allow the more progressive damage evolution as shown in Fig. 6, which is typical for polymer drops bonded to natural fibre. Frankl et al. [25] considered an incremental finite element model to study the delamination behaviour of an elastomer-matrix composite. This approach provides a higher degree of flexibility to predict non-linearities in the fibre microbond experiment. For instance, mechanical instabilities resulting from the crack propagation under frictional dissipation can be captured resulting in jaggedness of the force–displacement curves. This jaggedness is not observed in this study because individual flax fibres are used instead of bundles. Examples of composites that exhibit such jaggedness during tensile loading are mainly involving bundles of natural fibres such as bamboo, curauá, jute and sisal [24,37].

3.3. Numerical results: identification of interfacial parameters

The purpose of this part of the work is to predict the parameters of the interfacial debonding law that match the experimental evidence. According to the sensitivity analysis, the identification of the set of parameters is conducted sequentially by adjusting firstly the interfacial stiffness and the fibre–matrix complete separation displacement, and then the rest of the parameters follow. It has to be mentioned that the identification is conducted on each replicate from the five composites. Fig. 8 shows typical comparisons between the experimental and numerical responses for the selected replicates. This comparison highlights a nearly perfect matching obtained for all composites. It has to be mentioned that the ranking of IFSS of the studies composites does not necessarily reflect the maximum force levels illustrated in Fig. 8, because of the measurement of IFSS implies the knowledge of the fibre and microdroplet dimensions (i.e., Eq. 1).

Based on the identified behaviour implying five replicates per condition, the set of parameters of the interfacial debonding law are extracted, for which the average and standard deviation of all quantities are summarised in Table 2. Also, the predicted values of IFSS are shown with the percentage of scatter relative to the experimental values in Table 1. Based on IFSS measurements, flax fibre/PLA composite ranks as the top performing composite, followed by flax fibre/MAPP, flax fibre/PHA, flax fibre / PBS and then flax fibre/PP. This ranking promotes flax fibre/PLA interface as a high quality one.

The difference between experimental and numerical IFSS values expressed as a relative scatter percentage with respect to the experimental values (Δ_{IFSS}) demonstrates the fitness of the model in predicting the microdroplet test response with a great accuracy (Table 2). For all considered composites, the scatter is as small as 2%. Larger variability in microdroplet dimensions contrasts with the more stable fibre diameter for the replicates selected. This translates the difficulty to achieve similarity in microdroplet dimensions. As, this variability in microdroplet dimensions is implemented in the model, the predicted interfacial debonding parameters reflect the interfacial performance irrespective of dimensional considerations. The variability of the interfacial stiffness of all considered composites is acceptable knowing the low number of repetitions (i.e., five in total). The standard deviation evolves between 15% and 30% depending on the considered composite. The achieved scatter of the interfacial properties is related to the variability in fibre properties considered in the model through the use of five replicates for each composite. In addition, the interfacial stiffness does not vary significantly from one composite to another (between 47×10^9 and 59×10^9 N/m^3). The composite system that generates the highest interfacial stiffness is flax fibre/PHA (Table 2) The variability represents only 8% for the entire set of five composites. Larger variability is obtained for the maximum separation (δ_d) as the standard deviation varies between 12% and 39% with respect to the replicates. Even if the maximum separation represents a fraction of the microdroplet length (between 26% and 78% for the five studied composites), the predicted values are high and reflect the idea that the selected flax fibre/polymer composites trigger large shearing prior to rupture. The interpretation of debonding propagation rate (az) is difficult to achieve because of the short displacement interval during which fast force decay is recorded. This means that az exhibits a low sensitivity to some composite systems such as flax fibre/PBS or flax fibre/PLA. The variability of this parameter with respect to the number of replicates can still be considered as high as it reaches 54% in some cases. The identification of the non-linearity factor is facilitated by the variability in the observed trends especially the differences between the peak and the residual forces, which is affected by the nature of the composites. The standard deviation is found to vary between 7% and 32% with respect to the average value. In addition, if flax fibre/MAPP is excluded, f is found to vary near the value of 0.46, irrespective of the composite type. The analysis of the results shown in Table 2 can be used to assess the ranking of IFSS with respect to the interface properties irrespective of the matrix selection. This analysis shows that there is no clear trend between IFSS ranking and the interfacial stiffness. The same is true for the debonding propagation rate (a_z), and the non-linearity factor (f). However, there is a clear correlation between IFSS ranking and the maximum fibre–matrix separation displacement data (δ_d) that can be quantified using a linear function of the form

$$IFSS(\text{MPa}) = -0.57 + 0.1 \times \delta_d(\mu\text{m});\ R^2 = 0.96 \quad (4)$$

According to Eq. (4), there is a positive linear correlation between IFSS and the critical separation displacement irrespective of the composite system. It can be concluded that expression (4) suggests that among the set of interfacial parameters, the one that tunes the IFSS irrespective of the composite type is the critical separation displacement. Thus, the determination of this parameter allows a direct ranking of the composites according to IFSS criterion.

The predicted results in Table 2 are further discussed based on the literature available on simulation of pull-out of composites reinforced by natural fibres. To the best of the author knowledge, there is no equivalent work done on flax fibres according to the experimental setup and numerical scheme conducted in this study. Ferreira et al. [24] considered a 2D finite element simulation of the pull out test for varieties of natural fibres including Curauá, jute and sisal. Among the critical factors that affected the bond-slip predictions in their study is the geometric particularities of natural fibres and the relative humidity. In the present study, the humidity is kept constant for all experiments, which does not allow to conclude on the fibre shape modification on the interfacial behaviour. In addition, most of the simulations are performed with a limited fibre diameter variability representing only 13%. This means that scaling effect cannot be observed in a wide range of fibre dimensions. Despite this limitation, there seems to be a negative correlation between the interfacial stiffness and the fibre diameter. Another remarkable result is the positive correlation between the critical separation displacement and the fibre diameter, which cannot be verified from the simulation results of Ferreira et al. [24]. With regards to the robustness of the model to account for different possibilities of fibre adhesion improvement, Oushabi [38] invoked improving interfacial compatibility by chemical treatment of the fibre surface such as mercerization that has a tuning role of the surface roughness through mechanical interlocking. This role cannot be evaluated by the present model, which requires the implementation of a real fibre shape. This can be considered in a future work by implementing a 3D model of the flax fibre from X-ray micro-tomography results [39]. Another tuning role of chemical modification is the exposure of a larger part of cellulose on the surface of the fibre to increase the number of reaction sites. This role can be quantified from the present model by looking at the change in the interfacial stiffness and the critical separation displacement.

Scaling effects related to the microdroplet dimensions are not usually the focus of many research works fibre pull-out. This is the case for studies that do not use microdroplet configurations [35]. For those that develop setups similar to the present study, they dedicate more attention to the dimension variability of the natural fibres [24]. The effect of microdroplet dimensions can be tackled as a dependence of the mechanical behaviour on the contact area between the droplet and the blades. Because of the difficulty to control the droplet size, this effect cannot be accurately measured. As shown in Table 2, the variability of the droplet diameter ranges between 9% and 35% with respect to the average values and depending on the polymer type. From the simulation results shown in Table 2, scaling effect with respect to the droplet size are extracted from the individual replicates used for each polymeric system. Fig. 9 shows the results achieved for all interface parameters. The effect of droplet size on the interface interfacial stiffness ($K0z$) does not conclude on a prevailing tendency despite a scattered negative trend (Fig. 9a). The debonding propagation rate (az) has no remarkable dependence on the droplet size (Fig. 9b). However, the maximum fibre–matrix separation displacement(δ_d) seems to show the opposite trend compared to the interface interfacial stiffness (Fig. 9c). The non-linearity factor f shows the same scattered behavior as the debonding propagation rate.

4. Conclusions

This study demonstrates that developed finite element model of the microbond test predicts IFSS of polymeric drops bonded to flax fibre with deviation as small as 3% compared to the experimental values. This model proves that further exploitation of microdroplet tests is possible by implementing the interfacial behaviour under shear loading condition. The interfacial debonding model captures the diversity of interfacial behaviour exhibited by the polymeric drops bonded to flax fibre. The model captures either smooth or abrupt fibre pull out using four interfacial parameters: interfacial stiffness, maximum interfacial separation displacement, debonding non-linearity and decay rate. The interfacial stiffness for all tested composite between 47 and 59 GPa/mm is found to be negatively correlated to the flax fibre diameter. The flax fibre / PBS composite exbibits the largest interfacial stiffness due

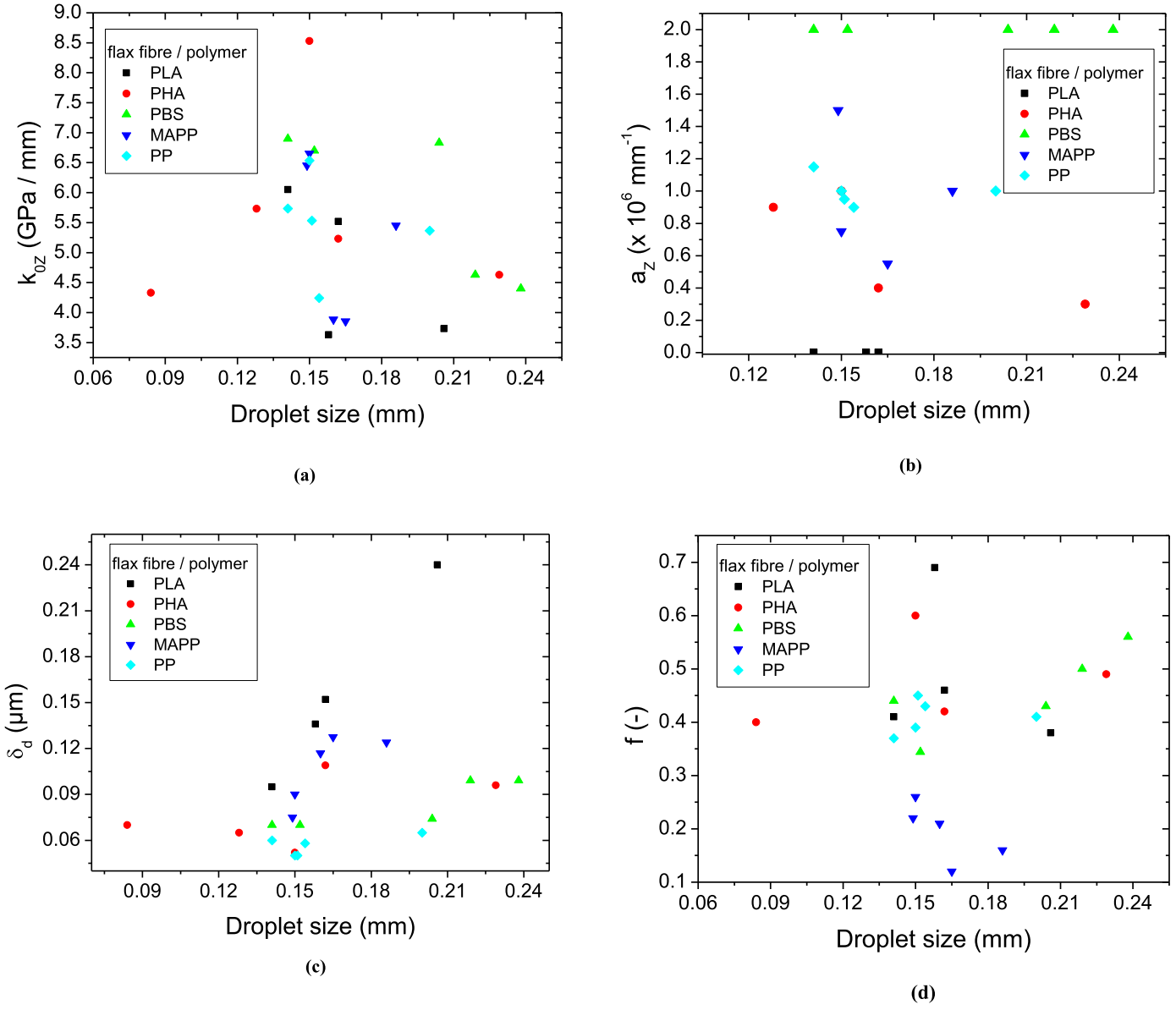

Fig. 9. Effect of droplet size on the interface parameters for all studied flax/polymer systems: (a) interfacial stiffness $K0z$, (b) debonding propagation rate az, (c) maximum fibre–matrix separation displacementδ_d, (d) non-linearity factor f.

probably to the large contact angle between PBS and flax fibre, which influences the adhesion through the wettability. The maximum interfacial separation displacement is found to vary in a large range between 57 and 156 μm depending on the composite system. The largest value is obtained for flax fibre / PLA composite allowing this system to achieve large shearing deformation prior to complete fibre pull out. Compatibility between flax fibre and PLA explains this result especially the presence of hydrogen bonds induced by the ester groups. Finally, this study concludes on the existence of a scaling law between the macroscopic pull-out test response and the local interfacial behaviour, which is materialised by the linear positive correlation between the IFSS and the maximum fibre–matrix separation displacement.

Declaration of Competing Interests

The authors declare the following financial interests/personal relationships which may be considered as potential competing interests:

Sofiane GUESSASMA reports financial support was provided by French National Institute for Agricultural Research INRAE. Sofiane GUESSASMA reports a relationship with French National Institute for Agricultural Research INRAE that includes: funding grants. Co-authors serving as guest editors for Composites Part C special issue Biobased composites

Data availability

Data will be made available on request.

Acknowledgements

The authors want to thank the INTERREG IV Cross Channel programme for funding this work through the FLOWER project (Grant Number 23). Antoine Kervoëlen (IRDL) is also thanked for his experimental contribution.

References

[1] BP Chang, AK Mohanty, M. Misra, Studies on durability of sustainable biobased composites: a review, RSC Adv. 10 (31) (2020) 17955–17999.
[2] D Pantaloni, D Shah, C Baley, A. Bourmaud, Monitoring of mechanical performances of flax non-woven biocomposites during a home compost degradation, Polym. Degrad. Stability 177 (2020) 109166-12.
[3] E Richely, A Bourmaud, V Placet, S Guessasma, J. Beaugrand, A critical review of the ultrastructure, mechanics and modelling of flax fibres and their defects, Progr. Mater. Sci. 124 (2021), 100851.
[4] D Notta-Cuvier, F Lauro, B. Bennani, An original approach for mechanical modelling of short-fibre reinforced composites with complex distributions of fibre orientation, Compos. Part A: Appl. Sci. Manuf. 62 (2014) 60–66.
[5] JC Zarges, P Sälzer, HP. Heim, Correlation of fiber orientation and fiber-matrix-interaction of injection-molded polypropylene cellulose fiber composites, Compos. Part A: Appl. Sci. Manuf. 139 (2020).
[6] J Beaugrand, S Guessasma, J-E. Maigret, Damage mechanisms in defected natural fibers, Sci. Rep. 7 (1) (2017) 14041-7.
[7] A Bourmaud, J Mérotte, D Siniscalco, M Le Gall, V Gager, A Le Duigou, et al., Main criteria of sustainable natural fibre for efficient unidirectional biocomposites, Compos. Part A: Appl. Sci. Manuf. 124 (2019) 105504-12.
[8] R. Koloor SS, MR Khosravani, RIR Hamzah, MN Tamin, FE model-based construction and progressive damage processes of FRP composite laminates with different manufacturing processes, Int. J. Mech. Sci. 141 (2018) 223–235.
[9] N Graupner, J Rößler, G Ziegmann, J. Müssig, Fibre/matrix adhesion of cellulose fibres in PLA, PP and MAPP: a critical review of pull-out test, microbond test and single fibre fragmentation test results, Compos. Part A: Appl. Sci. Manuf. 63 (2014) 133–148.
[10] A le Duigou, J Merotte, A Bourmaud, P Davies, K Belhouli, C. Baley, Hygroscopic expansion: a key point to describe natural fibre/polymer matrix interface bond strength, Compos. Sci. Technol. 151 (2017) 228–233.
[11] N Le Moigne, B Otazaghine, S Corn, H Angellier-Coussy, A Bergeret, Characterization of the Interface/Interphase in Natural Fibre Based Composites, in: Surfaces and Interfaces in Natural Fibre Reinforced Composites. SpringerBriefs in Molecular Science (BRIEFSMOLECULAR), Springer, Cham, 2018. https://doi.org/10.1007/978-3-319-71410-3_5.
[12] A le Duigou, A Bourmaud, E Balnois, P Davies, C. Baley, Improving the interfacial properties between flax fibres and PLLA by a water fibre treatment and drying cycle, Ind. Crops Prod. 39 (2012) 31–39.
[13] M Lilli, M Zvonek, V Cech, C Scheffler, J Tirillò, F. Sarasini, Low temperature plasma polymerization: an effective process to enhance the basalt fibre/matrix interfacial adhesion, Compos. Commun. 27 (2021) 100769-6.
[14] T Huber, U Biedermann, J. Müssig, Enhancing the fibre matrix adhesion of natural fibre reinforced polypropylene by electron radiation analyzed with the single fibre fragmentation test, Compos. Interfaces 17 (4) (2012) 371–381.
[15] PJ Herrera-Franco, A. Valadez-González, Mechanical properties of continuous natural fibre-reinforced polymer composites, Compos. Part A: Appl. Sci. Manuf. 35 (3) (2004) 339–345.
[16] Y Li, KL Pickering, RL. Farrell, Determination of interfacial shear strength of white rot fungi treated hemp fibre reinforced polypropylene, Compos. Sci. Technol. 69 (7-8) (2009) 1165–1171.
[17] JI Fajardo, J Costa, LJ Cruz, CA Paltán, JD. Santos, Micromechanical model for predicting the tensile properties of guadua angustifolia fibers polypropylene-based composites, Polymers 14 (13) (2022) 2627-17.
[18] PJ Herrera-Franco, LT. Drzal, Comparison of methods for the measurement of fibre/matrix adhesion in composites, Composites 23 (1) (1992) 2–27.
[19] PH. Petit, A simplified method of determining the inplane shear stress-strain response of unidirectional composites, Compos. Mater.: Testing Design (1969) 11–83. STP49808S.
[20] CC Chamis, JH. Sinclair, Ten-deg off-axis test for shear properties in fiber composites, Exp. Mech. 17 (9) (1977) 339–346.
[21] B Miller, P Muri, L. Rebenfeld, A microbond method for determination of the shear strength of a fiber/resin interface, Compos. Sci. Technol. 28 (1) (1987) 17–32.
[22] D Pantaloni, AL Rudolph, DU Shah, C Baley, A. Bourmaud, Interfacial and mechanical characterisation of biodegradable polymer-flax fibre composites, Compos. Sci. Technol. 201 (2021) 108529-8.
[23] KJ Wong, M Johar, SSR Koloor, M Petrů, MN. Tamin, Moisture absorption effects on mode II delamination of carbon/epoxy composites, Polymers 12 (9) (2020).
[24] SR Ferreira, RG Mendes de Andrade, E Koenders, F de Andrade Silva, E de Moraes Rego Fairbairn, RD. Toledo Filho, Pull-out behavior and tensile response of natural fibers under different relative humidity levels, Constr. Build. Mater. 308 (2021).
[25] S Frankl, M Pletz, C. Schuecker, Incremental finite element delamination model for fibre pull-out tests of elastomer-matrix composites, Proc. Struct. Integr. 17 (2019) 51–57.
[26] SSR Koloor, MA Abdullah, MN Tamin, MR. Ayatollahi, Fatigue damage of cohesive interfaces in fiber-reinforced polymer composite laminates, Compos. Sci. Technol. (2019) 183.
[27] A Le Duigou, P Davies, C Baley, Interfacial bonding of Flax fibre/Poly(l-lactide) bio-composites, Compos. Sci. Technol. 70 (2) (2010) 231–239.
[28] A Le Duigou, P Davies, C Baley, Exploring durability of interfaces in flax fibre/epoxy micro-composites, Compos. Part A: Appl. Sci. Manuf. 48 (2013) 121–128.
[29] F Teklal, A Djebbar, S Allaoui, G Hivet, Y Joliff, B. Kacimi, A review of analytical models to describe pull-out behavior – Fiber/matrix adhesion, Compos. Struct. 201 (2018) 791–815.
[30] M Frikha, H Nouri, S Guessasma, F Roger, C Bradai, Interfacial behaviour from pull-out tests of steel and aluminium fibres in unsaturated polyester matrix, J. Mater.Sci. 52 (24) (2017) 13829–13840.
[31] S Rjafiallah, S. Guessasma, Three-phase model and digital image correlation to assess the interphase effect on the elasticity of carbohdyrate polymer-based composites reinforced with glass silica beads, Carbohyd. Polym. 83 (1) (2011) 246–256.
[32] S Rjafiallah, N Benseddiq, S. Guessasma, Effect of interface properties on the effective properties of biopolymer composite materials, Mater. Werkst 41 (5) (2010) 265–269.
[33] L Marrot, A Bourmaud, P Bono, C. Baley, Multi-scale study of the adhesion between flax fibers and biobased thermoset matrices, Mater. Des. 62 (2014) 47–56 (1980-2015).
[34] E Pisanova, S Zhandarov, E. Mäder, How can adhesion be determined from micromechanical tests? Compos. Part A: Appl. Sci. Manuf. 32 (3-4) (2001) 425–434.
[35] J Zhou, Y Li, N Li, X Hao, C. Liu, Interfacial shear strength of microwave processed carbon fiber/epoxy composites characterized by an improved fiber-bundle pull-out test, Compos. Sci. Technol. 133 (2016) 173–183.
[36] S Bahl, AK. Bagha, Finite element modeling and simulation of the fiber–matrix interface in fiber reinforced metal matrix composites, Mater. Today: Proc. 39 (2021) 70–76.
[37] X Gao, D Zhu, S Fan, MZ Rahman, S Guo, F. Chen, Structural and mechanical properties of bamboo fiber bundle and fiber/bundle reinforced composites: a review, J. Mater. Res. Technol. 19 (2022) 1162–1190.
[38] A. Oushabi, The pull-out behavior of chemically treated lignocellulosic fibers/polymeric matrix interface (LF/PM): a review, Compos. Part B: Eng. 174 (2019).
[39] E Richely, S Durand, A Melelli, A Kao, A Magueresse, H Dhakal, et al., Novel insight into the intricate shape of flax fibre lumen, Fibers 9 (4) (2021) 24.